International Journal for Housing Science and Its Applications
Publish August 5, 2025. Volume 46, Issue 3 Pages 4133-4143

https://doi.org/10.70517/ijhsa463353

Research on Precision Operation Control System for Agricultural Machines Based on Enhanced Target Detection Algorithm

Xiuni Li[1,*]
[1] Xi'an Kedagaoxin University, Xi'an, Shaanxi, 710000, China
Corresponding authors: (e-mail: HHxx201320@163.com).

Abstract This paper takes a harvester as an example to analyze the components of a precision operation control system for agricultural machines. A target detection model (SSD) is introduced for pedestrian detection in the farmland environment. The SSD-Mobilenet network model is used to improve the detection real-time. Further fusion of Feature Pyramid Network (FPN) realizes multi-scale feature extraction for detecting targets and enhances target detection accuracy. Design a depth sensor-based combination of far and near field stubble multi-information detection scheme to improve the accuracy and stability of agricultural land environment detection. Verify the effectiveness of the method in this paper through model training and simulation experiments, etc. The results show that the threshold value is set to 0.55, and the sensor detection effect is the best. In the model training, the value of the intersection and merger ratio is close to 1, and the loss value is close to 0. The enhanced target detection algorithm has a higher recognition effect than the 2 comparative algorithms in all 6 types of pedestrian states. In the special scene simulation experiments, the average reward value of this paper's algorithm is finally stabilized in the interval of 0.1 to 0.3, and the path length is stabilized at about 100 steps with less fluctuation, and the precise operation assistance effect is better than the comparison algorithm.

Index Terms enhanced target detection, feature pyramid network, multi-scale feature extraction, pedestrian detection on agricultural land, precision operation of agricultural machines

I. Introduction

Under the national strategic background of increasing level of mechanization of agricultural production and rapid development of urbanization, land transfer has accelerated and large-scale farms have become the direction of development [1], [2]. While pursuing efficiency improvement of agricultural machinery operation, farm managers need to strictly control the operation quality [3]. However, traditional agricultural machinery is limited by manual operation, high labor intensity, the quality of operation is completely dependent on the skills of the driver, and field night operation is basically unattainable [4]-[6]. In addition, affected by the current situation of agricultural non-structural production environment and the shortage of professional operators of agricultural machinery, the performance of traditional agricultural machinery can no longer meet the actual production needs [7], [8]. At present, unmanned farms supported by intelligent farm machinery are being constructed at an accelerated pace, and the precision operation control system of farm machinery is in urgent need of further breakthroughs under the new mode of unmanned autonomous farm machinery operation.

Precision agriculture is the main development trend of modern agriculture worldwide [9]. Its core guiding idea is to use satellite global positioning system, geographic information system and remote sensing technology to obtain the spatial and temporal differences of various factors affecting the growth and yield of crops in the farmland, and adopt targeted field operation measures to avoid the waste of resources and environmental pollution caused by blind inputs into the farmland, and to improve the yield and quality of the crops at the same time [10]-[13]. Meanwhile, intelligent algorithms are one of the key technologies to realize agricultural precision operations. Taking agricultural equipment as a carrier, based on the intelligent algorithm's intelligent perception of the operating status of agricultural machinery, crop, soil, environment and other information, shared by data transmission, the decision-making model is constructed, so as to guide the precise monitoring and intelligent management of agricultural equipment and promote the development of agricultural machinery intelligence [14]-[17]. It can free drivers from heavy work, reduce fatigue, improve productivity and maneuvering safety, and have a significant role in promoting the realization of the intelligence of China's agricultural machinery and the precision of agricultural production [18]-[20].

The intelligent development of agriculture cannot be separated from the accurate recognition and harvesting of agricultural objects supported by intelligent algorithms. In this paper, from the design of sensors and control units, etc., an enhanced target detection algorithm is introduced into the system to improve the accuracy of pedestrian and agricultural object detection of the harvester. The combination of Mobilenet network and feature pyramid network (FPN) with the target detection algorithm is utilized to improve the detection effect. The stubble multi-information detection scheme combining far and near views is used to improve the accurate environment detection and agricultural objects harvesting under the autonomous navigation of the harvester. Combined with simulation experiments and other analyses, we analyze the optimization effect of this paper's method in the precision operation control system of agricultural machines.

II. Technical analysis of precision operation control system for harvester

This chapter systematically elaborates the harvester-related hardware design, introduces target detection algorithms and depth sensors, etc., to realize the harvester's precise recognition of agricultural targets and detection of harvesting and so on.

II. A. Harvester hardware design

II. A. 1) Sensor selection and layout

The decision on sensor selection and layout is based on factors such as operating environment, specific system requirements and cost-effectiveness. The vision sensor model is Hikvision DS-2CD2085G1-i, which provides image data with 1920×1080 resolution and 35fps frame rate, and is set in the front of the machine to observe the crop and terrain; the GPS module is selected from the Beidou Satellite Navigation Module, which provides accurate centimeter-level positioning data, and is set on the top of the machine to ensure a smooth signal; the laser radar (LiDAR) DJI Livox Horizon is used for high-resolution 3D scanning and obstacle detection, which is set around the machine; and Kobelco K50 is used for temperature and humidity sensors, which monitors the temperature and humidity of the operating environment, and is set around the machine.

II. A. 2) Control units and actuators

In the hardware design of the control unit and actuators, the central control unit adopts Huawei Kunpeng 920 processor, and the motor controller selects MCAC706, which is suitable for high-precision control and supports precise speed and position control. The servo drive is Siemens V90 for precise control of motor movement; the sensor interface of the actuator is CONTRINEX sensor/actuator S12 wiring connector S12-4FNG-000-NNT3, which ensures fast and reliable data exchange and synchronized control.

II. B. Improved model design based on target detection algorithm (SSD network)

II. B. 1) Introduction to the SSD model

The task scenarios need to be considered in the model design: 1) Due to the complexity of the farmland scene, there are squatting or lying pedestrian application scenarios for the pedestrian detection task, and there is a demand for small target detection. 2) Pedestrians are mostly moving targets, which still require high real-time detection capability on hardware devices with low-computer power for reasoning. 3) A high target detection accuracy is required. Considering the above three points, SSD series model can well meet the demand.

SSD model is a single-stage detector based object detector with the advantage of miniaturization compared to other deep learning models.SSD models usually have fewer parameters and computational requirements, so they can be run on edge devices more easily. It also has fast detection speed and high accuracy. On edge devices, the advantage of processing speed can help in fast detection and response in real-time applications. Since SSD models are relatively small, they have lower computation and storage requirements and low power consumption for daily operation, which can reduce energy consumption and extend device battery life.

II. B. 2) SSD model improvement

To reduce the computational complexity of the SSD-VGG16 detector, the Mobilenet network model is used to replace the VGG16 network to improve the real-time performance of the SSD detector. The second-generation Mobilenet network model (i.e., MobilenetV2) is selected as the backbone network model for the SSD detector.The SSD-MobilenetV2 detector follows the design of the SSD-VGG16, and the front-end MobilenetV2 network employs six feature maps of different sizes for the back-end detection network to perform multi-scale target detection. There are some problems with the SSD-MobilenetV2 detector due to the change of the backbone network from VGG-16 to MobilenetV2.

A comparison of the size of the multilayer feature maps extracted by the SSD-VGG16 and SSD-MobilenetV2 backbone networks reveals that the size of the feature map extracted by the MobilenetV2 network in the first layer

is half of that of the VGG16 network, which makes the target detection range of the MobilenetV2 network only half of that of the VGG16 network in terms of the corresponding feature maps, leading to its lower detection accuracy in practical applications. On the other hand, the 38x38 feature maps provided by the MobilenetV2 network are shallow features, making it difficult to extract effective image feature maps. In this study, we try to use the FPN module to fuse the output feature maps of the MobilenetV2 network to improve the detection accuracy without adding too many parameters.

FPN is a feature pyramid network for target detection and semantic segmentation tasks and is a multi-scale feature extraction network architecture. The basic idea is to use deep convolutional neural networks to extract multi-scale features, transfer and aggregate information through cross-layer connections, and generate feature pyramids with different resolutions to better adapt to objects of different scales and improve the performance of target detection and semantic segmentation tasks. The introduction of FPN in the target detection task can improve the target recognition accuracy, the traditional target detection method uses a single scale feature map, the small target is weakly represented on the feature map, which can easily lead to the small target missed detection or inaccurate detection, while FPN constructs the pyramid structure, extracts image feature maps at different levels, generates multi-scale feature maps, and the different levels of feature maps correspond to different scales of the target objects, which can effectively improve the detection accuracy of the small target, and also integrates different scales of objects through feature fusion. Different levels of feature maps correspond to different scales of target objects, which can effectively improve the small target detection accuracy, and also integrate different levels of feature information through feature fusion to get more accurate target detection results.

The FPN architecture consists of a backbone network and a top network. Figure 1 shows the principle of FPN. The backbone network is used to extract the original image features, and then down-sampling and up-sampling operations are performed in the top network to generate multi-scale feature pyramids. In the down-sampling process, the feature map size gradually decreases and the number of channels gradually increases; in the up-sampling process, the feature map size gradually increases and the number of channels gradually decreases. Eventually, feature maps of different scales are integrated together to form feature pyramids with different resolutions.

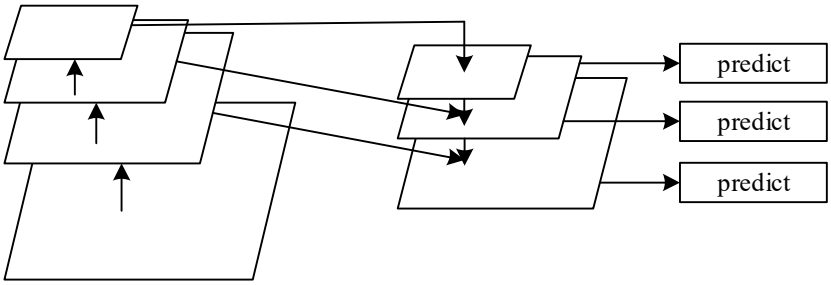

Figure 1: Principle of FPN

The mathematical principle of FPN can be expressed by the following equations:

(1) Bottom-up feature extraction:

$$(C_1, C_2, C_3, C_4, C_5) = backbone(I) \tag{1}$$

The bottom-up feature extraction principle is shown in Equation (1), where I is the input image and C_i denotes the feature map of the i th convolutional layer. SSD-MobilenetV2 is used as backbone network.

(2) Top-down feature pyramid:

$$P_5 = top - down(C_5) \tag{2}$$

$$P_i = upsample P_{i+1} + lateral(C_i), i = 4, 3, 2, 1 \tag{3}$$

The top-down feature pyramid formulation is shown in (2), (3). Where P_i denotes the i th layer of pyramid features, top-down denotes the top-down feature upsampling operation, upsample denotes the bilinear interpolation upsampling operation, and lateral denotes the bottom-up feature fusion operation.

(3) Target detection

Finally, a target detection algorithm is applied on the fused pyramid feature map for target detection.FPN mainly extracts semantic information from different scale feature maps and fuses them for target detection through bottom-up and top-down approaches. Specifically, bottom-up feature extraction extracts multi-scale feature maps, top-down

feature pyramid fuses these feature maps, and finally the target detection algorithm performs target detection on the fused feature maps.

II. C.Depth sensor-based multi-information detection of cut stubble

II. C. 1) Operational conditions for autonomous navigation of harvesters

The harvester mainly consists of two basic functions, i.e. traveling function and harvesting function, especially the harvesting function makes the harvester become one of the most important agricultural harvesting machines. The traditional harvester in the operation process, the driver needs to observe the crop in the field of a variety of characteristics of information, such as crop operation boundary, fall and growth, etc., the driver with experience to complete the harvester's direction of travel, speed and height of the cutting platform and other operations, in order to improve the harvest quality of the harvester.

For the driverless harvester autonomous operation, the ultimate goal is to be able to replace the manual driving at the same time to ensure the quality of harvesting and operational efficiency. In order to realize the autonomous operation of the harvester in the field, it is not enough to study the unmanned operation of the harvester body, and it should be combined with the demand for harvesting operations, and it should also make real-time detection and feedback of the field crops while realizing the unmanned operation of the harvester body, and improve the autonomous harvesting function, so as to realize the precise operation of the harvester.

Therefore, based on the premise of this design goal, while studying the unmanned driver problem of the harvester, the research on grain feature detection during its autonomous operation is also crucial.

II. C. 2) Combined near and far view stubble multi-information detection program design

In order to realize the autonomous operation of combine harvester in the field, this paper designs a depth sensor-based stubble multi-information detection scheme combining far and near views. Figure 2 shows the top view of the depth sensor arrangement relationship.

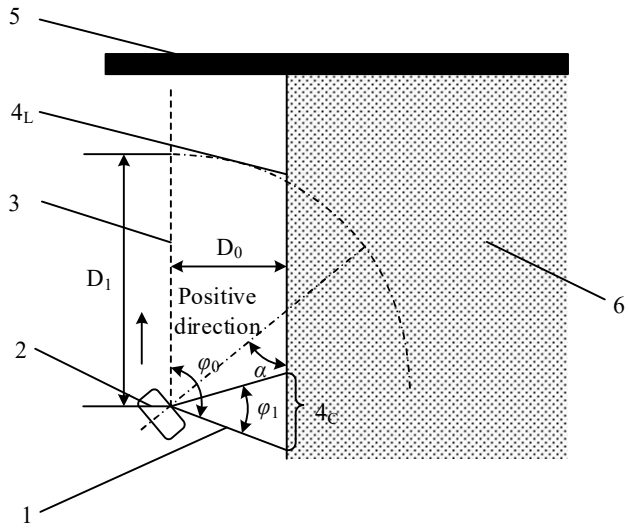

1. horizontal field of view rear edge line, 2. depth sensor,
3. horizontal field of view front edge line, 4_L. stubble line,
4_C. stubble proximity area, 5. lateral ridge, 6. grain

Figure 2: Top schematic diagram of arrangement relationship of depth sensors

According to the depth sensor characteristics and harvester autonomous operation detection needs, the combine harvester harvesting operation should satisfy the following relationship equation:

$$D_0 \le D_1 \tag{4}$$

$$\alpha = \frac{1}{2}\varphi_0 \tag{5}$$

Eq, D_1 - is the vertical distance between the depth sensor and the stubble cut boundary line, m, D_1 - is the minimum effective depth detection threshold of the depth sensor, m, α - is the angle between the horizontal

viewing direction of the depth sensor and the longitudinal centerline of the combine body, °, φ_0 - is the horizontal field of view range of the depth sensor, °, φ_1 - is the near field of view range, °.

The left line of the horizontal field of view of the depth sensor in the figure should be parallel to the operation direction of the combine, where φ_0 is the horizontal field of view angle of 91.3°.

The stubble multi-information detection method combining the near and far view is specified as follows: the depth sensor completes the identification of the spike head region and the fallen region in the near view detection range 4_C, and obtains a certain length of stubble boundary line information as well as a lateral ridge in the far view range, and guides the combine harvester to accurately travel to complete the harvesting operation of the crop.

To further determine the optimal installation height and angle of the depth sensor, and to consider the effect of actual field illumination, Figure 3 shows the specific experimental image acquisition process.

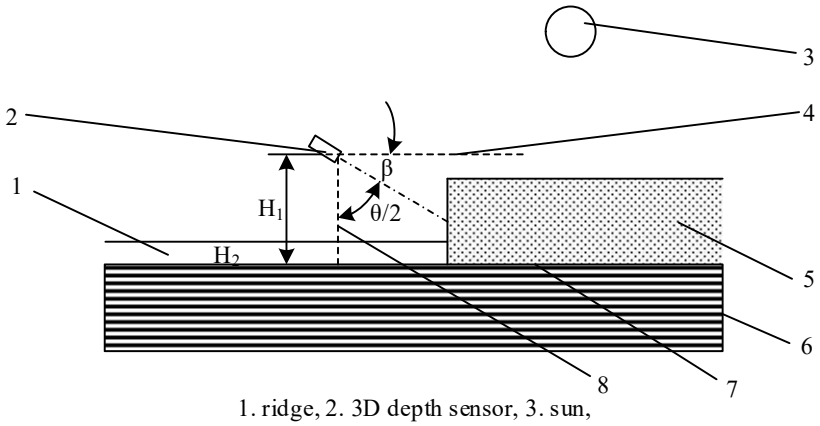

1. ridge, 2. 3D depth sensor, 3. sun,
4. upper edge of vertical field of view, 5. grain, 6. ground,
7. crop stubble line, 8. lower edge of vertical field of view

Figure 3: Side view of the arrangement relationship of the depth sensor

According to the characteristics of the depth sensor and the harvester's autonomous operation detection needs, the height of the depth sensor from the ground should be maintained at more than double the height of the plant and less than double the height of the plant, with the following relational equation:

$$[H] \le H_1 \le 2[H] \tag{6}$$

$$\beta = 90^{\circ} - \frac{1}{2}\theta_0 \tag{7}$$

Eq, H_1 - is the height of the depth sensor above the ground, m, $[H]$ - is the maximum plant height of the applicable grain for the harvester, m, β - is the downward tilt angle of the vertical framing direction of the depth sensor, °, θ_0 - is the vertical field of view range of the depth sensor, °.

The lower edge line of the vertical field of view of the depth sensor in the figure should be perpendicular to the ground, where θ_0 is the vertical field of view angle of 65.7°.

According to the above design scheme of horizontal and vertical installation of the depth sensor, it can ensure that it can effectively obtain the 4_L information of the stubble line and the information of the horizontal field ridge, and effectively reduce the interference of redundant information caused by the large field of view, as well as avoiding the direct exposure of sunlight on the lens of the sensor, which improves the accuracy and stability of the depth detection in a large field environment.

Because the depth camera detects a three-dimensional three-dimensional space, it is also necessary to establish a three-dimensional coordinate system model to analyze the relative positional relationship between the machine-camera-crop when determining the specific installation location. Figure 4 shows the depth sensor coordinate system model.

The reference coordinate system of the depth camera can be expressed as:

$$R = (O, Ox, Oy, Oz) \tag{8}$$

where O is the origin of the coordinate system, usually the harvester carries the depth camera along the direction of Oz, in the reference coordinate system, the angle between the infrared beam projected by the depth sensor and the Ox axis is θ, the depth data measured by the depth sensor can be expressed in the transverse plane coordinate system as (ρ,θ), then its conversion relationship with the two-dimensional right-angle coordinate system is as follows:

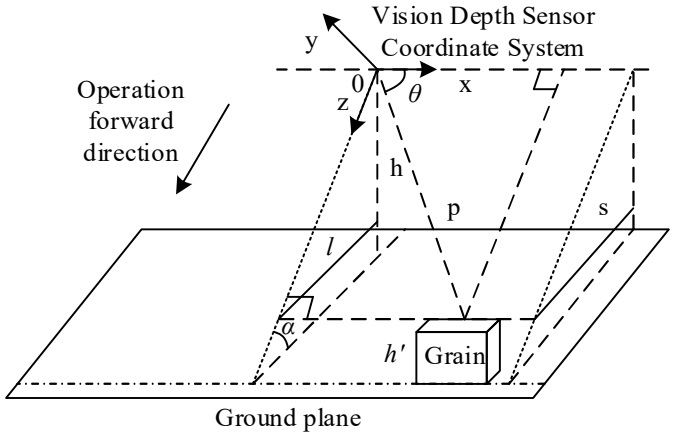

Figure 4: Depth sensor coordinate system model

$$\begin{bmatrix} x \\ y \\ z \end{bmatrix} = \begin{bmatrix} \rho \cdot \cos\theta \\ 0 \\ \rho \cdot \sin\theta \end{bmatrix} \tag{9}$$

Its positional relationship satisfies the following relational equation:

$$s = \frac{h}{\sin\alpha} \tag{10}$$

Eq, S - is the distance between the depth camera and the ground along the Oz axis, m, H - is the mounting height of the depth camera relative to the ground, m, α - is the installation pitch angle of the depth camera, °.

According to the above three-dimensional coordinate system model of the relationship between the parameters, the relevant data into the relationship equation can be roughly deduced the optimal installation height and pitch angle of the sensor.

III. Effectiveness check of enhanced target detection algorithm

In this chapter, the proposed enhanced target detection algorithm is tested through multiple sets of experiments to analyze the value of the algorithm in supporting precision operations of agricultural machines.

III. A. Algorithm Detection and Recognition Effect Validation

III. A. 1) Effect of threshold on detection results

The setting of the threshold value has a large impact on the detection effect of the depth sensor, and it is crucial to choose the best threshold value. In this section, a comparison of the detection effect is carried out by setting different thresholds to determine the optimal threshold for the model in this paper. The default threshold value is 0.55. When the threshold value is below 0.35, the change of the improved enhanced target detection model is very insignificant, and when the threshold value is greater than 0.75, the improved enhanced target detection model will be greatly affected, and the leakage detection rate is greatly increased. So in this section, the threshold range is limited to between 0.35 and 0.75 for the comparative analysis of detection results.

Table 1 shows the detection results under different thresholds. From Table 1, it can be concluded that the optimal threshold value is 0.55, when the threshold value is 0.55, the model's detection rate for agricultural commodities is as high as 96.29%, the detection rate is 91.28%, and the reconciliation mean F_1 is 93.18%, and the data of the three indexes are better than that under other comparative thresholds. Therefore, in this paper, the optimal threshold of the model is set to 0.55.

Table 1: Test results under different thresholds

Thresholds	P(%)	R(%)	F_1(%)
0.35	94.61	89.21	91.33
0.45	95.42	90.53	92.02
0.55	96.29	91.28	93.18
0.65	95.60	88.20	91.61
0.75	93.23	84.22	87.31

III. A. 2) Interchange and integration ratio (IOU)

The IOU (intersection and concordance ratio) of the predicted frame to the true frame needs to be calculated in the agrochemical detection experiment. It is generally considered that as long as the following conditions are met is the correct detection result, called a positive sample. Ideally, the IOU value is 1. This situation proves that the manually labeled true frame and the predicted frame of the detection model are completely overlapped, i.e., the detection model performs well.

$$IOU = \frac{Area\ of\ Overlap}{Area\ of\ Union} \geq 0.55 \tag{11}$$

In the experimental process, the improved target detection algorithm is used by training on the publicly available crop dataset, exporting the output training logs and parsing their data, calculating the intersection and concurrency ratio of the real frame and the predicted border, recording the value of IOU for each 1 iteration, and drawing the change curve of IOU. Figure 5 shows the convergence of the IOU curve. The horizontal coordinate indicates the number of iterations, and the maximum number of iterations set is 45000. The vertical coordinate is the value of IOU, and the closer to 1 represents the higher accuracy of the model. After 29849 iterations of the target curve in Figure 5, the IOU value is basically stabilized above 0.987, close to 1, and the change is not large, which meets the requirement of high accuracy of target detection.

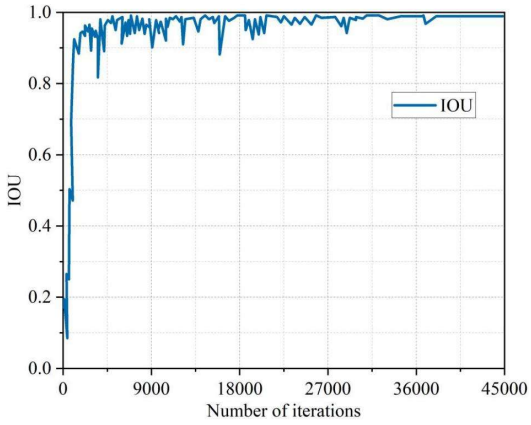

Figure 5: The convergence of the IOU curve

III. A. 3) Loss function

According to the training log, the change of the loss function of the improved target detection algorithm model is obtained. Figure 6 shows the loss value function curve during network training, the vertical coordinate indicates the loss value, the horizontal coordinate indicates the number of iterations, and the maximum number of iterations is set to 45000 times. As can be seen in Figure 6, the loss value is decreasing with the increase of iteration number, when the network iteration is more than 36000 times, the loss value change is basically stable, and finally the loss value decreases to 0.035, which is very close to 0. From the point of view of the convergence situation, the network training result meets the requirements, and the depth sensor that introduces the enhanced target detection algorithm can be mounted on the harvester, and be used in the actual agricultural object detection and harvesting situations.

III. A. 4) Recognition results under different pedestrian states

In order to judge that the target detection algorithm introducing FPN has better pedestrian detection performance, the algorithm before and after the improvement is subjected to comparison experiments of detection and recognition under different pedestrian states. Table 2 shows the comparison of the recognition results under different pedestrian states. The improved target detection algorithm has a detection rate of 98.26% in large targets and 94.27% in full

targets, which is 1.37% and 0.87% respectively compared with the pre-improvement algorithm; the improved target detection algorithm has a detection rate of 96.59% in medium targets and 90.36% in full targets, which is 2.28% and 1.74% respectively compared with the pre-improvement algorithm; the improved target detection algorithm has a detection rate of 2.28% and 1.74% respectively compared with the pre-improvement algorithm. 1.74%; the improved target detection algorithm has a detection rate of 94.35% and a completeness rate of 87.68% for small targets, which are 2.25% and 7.26% higher than the pre-improvement rate, respectively. The improved target detection algorithm has a detection rate of 99.37% in unobstructed targets and a detection rate of 98.09% in full targets, which are 1.16% and 3.78% higher than before; the improved target detection algorithm has a detection rate of 96.39% in less obstructed targets and a detection rate of 92.16% in full targets, which are 3.16% and 3.86% higher than before; the improved target detection algorithm has a detection rate of 94.35% in small targets and a detection rate of 87.68% in full targets, which are 2.25% and 7.26% higher than before. The improved target detection algorithm has a detection rate of 93.27% and a full detection rate of 87.65% for multi-obstructed targets, which are 2.05% and 7.14% higher than the pre-improvement rate, respectively. We can conclude from this that the improved target detection model has improved the recognition results in different pedestrian states compared with the pre-improvement period, and can more accurately and comprehensively recognize the actual farmland situation in complex harvester operation scenarios.

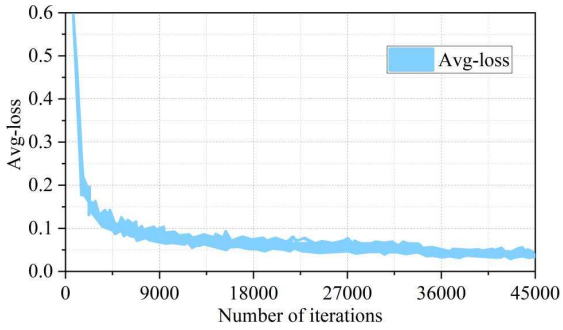

Figure 6: Loss function curve

Table 2: Identification results under different agricultural product states

Category	Model	P(%)	R(%)	F_1(%)
Big target	Before improvement	96.89	93.40	94.81
	After improvement	98.26	94.27	96.09
Middle target	Before improvement	94.31	88.62	91.00
	After improvement	96.59	90.36	92.37
Small target	Before improvement	92.10	80.42	86.31
	After improvement	94.35	87.68	91.16
No obstruction	Before improvement	98.21	94.31	96.52
	After improvement	99.37	98.09	98.78
Less obstruction	Before improvement	93.23	88.30	91.21
	After improvement	96.39	92.16	94.27
Multiple obstructions	Before improvement	91.22	80.51	86.22
	After improvement	93.27	87.65	90.19

III. B. Path Planning Simulation Experiments for Special Scenarios

III. B. 1) Training Average Reward Value and Path Planning Length for the Algorithm in this Paper

The special agricultural scenarios in this paper mainly focus on two types of farmland layouts, “I” and “U”, which have a high risk of deadlock for mobile devices, thus preventing them from reaching the predetermined location and realizing the harvesting of agricultural products. In order to test that the enhanced target detection algorithm in this paper can successfully recognize the farmland layout, avoid the mobile device from falling into a deadlock state, and try to stay away from the potentially dangerous areas, simulation experiments are set up to shorten the training cycle in such environments, so that the model can reach a stable state more quickly.

The model is trained in special scenarios and the average reward value obtained by the model in each iteration with the length of path planning is recorded. Figure 7 shows the average reward value and path planning length of the model trained in special scenarios. The left side of Fig. 7 shows the average reward for each round of training, and analyzing the change of the average reward, it can be found that after 57 rounds of iterations, the average

reward rises from the initial -0.151 or so to more than 0; after 140 rounds of iterations, the average reward value stabilizes in the interval from 0.1 to 0.3; throughout the iteration process, the average reward has been showing an upward trend and the fluctuation is gradually reduced, and finally reached a stable state. The right side of Fig. 7 shows the path length of each planning, in the initial stage, because the model has not yet fully mastered enough experience in breaking away from deadlocks, the path length fluctuates greatly between 50 and 250 steps, and the longest is almost close to 250 steps; however, with the deepening of the training and accumulation of experience in the model, the path length gradually stabilizes at about 100 steps, and the fluctuation amplitude is also significantly reduced. The experimental results show that the introduction of the enhanced target detection model in mobile devices can effectively guide the mobile devices to learn how to get out of the deadlock region, and make the algorithm eventually stabilize, so that the average reward value and path length are maintained in a good interval.

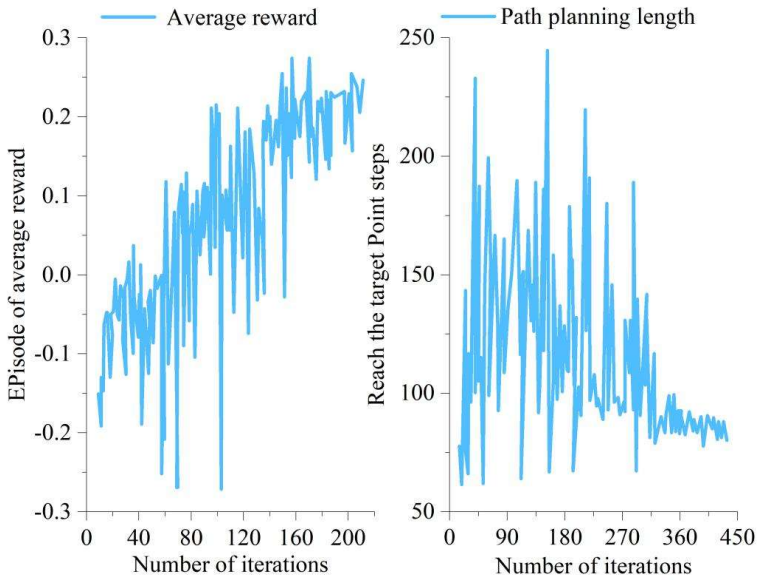

Figure 7: Average reward value and path planning length of training

III. B. 2) Comparison of training path planning lengths for different algorithms

Take the training path planning length as an example to compare the path planning effect of different algorithms. The basic PPO algorithm and an improved SDAS-PPO algorithm with better results based on the PPO algorithm are chosen to be compared with this paper's algorithm, and experiments are carried out under the scenarios of special obstacle layouts and mixed obstacle layouts.The SDAS-PPO algorithm introduces importance sampling technology and experience playback mechanism, and optimizes the process of action selection through the assistance of the selfdirected network, so as to make more accurate action decisions in the complex environments. to make more accurate action decisions in complex environments.

Fig. 8 shows the comparison of the training generated path lengths of each algorithm in an obstacle environment with special layout. From Fig. 8, it can be observed that the algorithms in this paper show smaller and more stable step lengths than the basic PPO algorithm and the SDAS-PPO algorithm at the beginning of training, basically in the range of 60-250 steps. After a certain number of rounds of training, the PPO algorithm shows some progress, but its performance still has large fluctuations, and even in the late stage of training, the step size still remains above 90 steps.The SDAS-PPO algorithm also has higher volatility than this paper's algorithm, with the highest almost approaching 400 steps. Compared with this paper's algorithm, the comparison algorithm is still insufficient in terms of stability and path planning effect. This comparison result fully proves that this paper's algorithm has an advantage in path planning compared with other comparison algorithms, and can better assist the precise operation of agricultural machinery.

III. C. Comparison of Training Average Reward Value and Path Planning Length in Mixed Scenarios

Fig. 9 shows the comparison of the average reward values of the basic PPO algorithm, SDAS-PPO algorithm and this paper's algorithm for each round of training in the mixed layout obstacle environment. Through comparative analysis, although the average rewards of these three algorithms are kept around 0.0 to 0.2 in steady state, the base PPO and SDAS-PPO algorithms are more volatile, while the algorithm in this paper performs more stably. Figure 10 shows the comparison of the path lengths of the three algorithms after each path planning. Through comparative analysis, this paper's algorithm is basically stable between 80-90 steps after 450 iterations, and is

better than the basic PPO algorithm and SDAS-PPO algorithm in terms of convergence speed and stability. The experimental results prove that the algorithm in this paper has advantages in robustness and generalization ability, and can provide a more stable and reliable path planning solution in diverse farmland environments to realize the accurate harvesting of agricultural objects by harvesters.

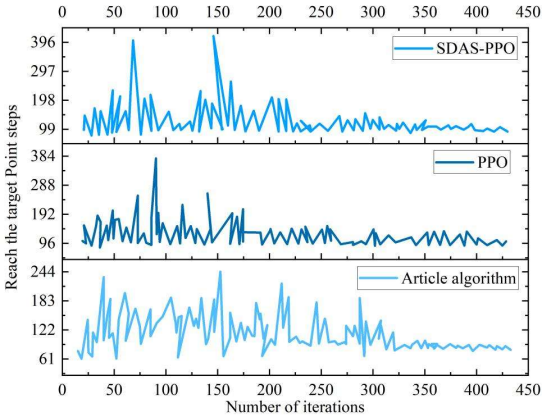

Figure 8: Comparison of path planning length in special scenarios

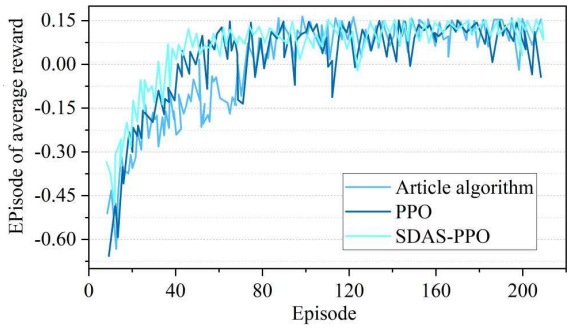

Figure 9: The average reward value of training in mixed scenarios

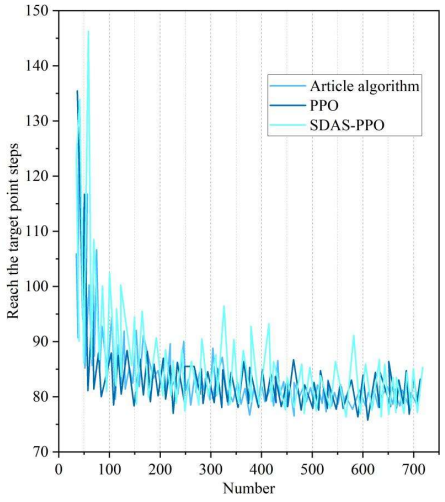

Figure 10: Path planning length in mixed scenarios

IV. Conclusion

In this paper, an enhanced target detection algorithm is applied to improve the harvester's ability to autonomously navigate and harvest agricultural materials for precise operation control. The threshold value is set to 0.55, which can obtain the highest 96.29% detection rate, 91.28% detection rate, 93.18% reconciled mean F_1. The intersection and merger ratio and the loss function prove that this paper's algorithm has a high recognition accuracy. Under the

six types of pedestrian states, this paper's algorithm can achieve the highest recognition accuracy of 99.37% and 98.09%. The training average reward value and path planning length of this paper's algorithm in special and mixed scenarios indicate that the use of this paper's algorithm can assist the harvester to realize stable and accurate detection of the farmland environment and harvesting of agricultural materials. In the future, we can explore how to introduce the recognition error reporting mechanism in the algorithm to provide timely farmland environment warning for monitors and reduce the possibility of damage during the automated and precise operation of agricultural machines.

References

[1] Wang, S., Bai, X., Zhang, X., Reis, S., Chen, D., Xu, J., & Gu, B. (2021). Urbanization can benefit agricultural production with large-scale farming in China. Nature Food, 2(3), 183-191.

[2] Ren, C., Liu, S., Van Grinsven, H., Reis, S., Jin, S., Liu, H., & Gu, B. (2019). The impact of farm size on agricultural sustainability. Journal of Cleaner Production, 220, 357-367.

[3] Mentsiev, A. U., Amirova, E. F., & Afanasev, N. V. (2020, August). Digitalization and mechanization in agriculture industry. In IOP Conference Series: Earth and Environmental Science (Vol. 548, No. 3, p. 032031). IOP Publishing.

[4] Peng, J., Zhao, Z., & Liu, D. (2022). Impact of agricultural mechanization on agricultural production, income, and mechanism: evidence from Hubei province, China. Frontiers in Environmental Science, 10, 838686.

[5] Sims, B., & Kienzle, J. (2017). Sustainable agricultural mechanization for smallholders: What is it and how can we implement it?. Agriculture, 7(6), 50.

[6] Özpınar, S., & Çay, A. (2018). The role of agricultural mechanization in farming system in a continental climate. Tekirdağ Ziraat Fakültesi Dergisi, 15(2), 58-72.

[7] Lu, F., Meng, J., & Cheng, B. (2024). How does improving agricultural mechanization affect the green development of agriculture? Evidence from China. Journal of Cleaner Production, 472, 143298.

[8] Qiao, F. (2017). Increasing wage, mechanization, and agriculture production in China. China Economic Review, 46, 249-260.

[9] Monteiro, A., Santos, S., & Gonçalves, P. (2021). Precision agriculture for crop and livestock farming—Brief review. Animals, 11(8), 2345.

[10] Yousefi, M. R., & Razdari, A. M. (2015). Application of GIS and GPS in precision agriculture (a review). International Journal of Advanced Biological and Biomedical Research, 3(1), 7-9.

[11] Zhmud, V. A., & Dimitrov, L. (2017). Designing of the precision automatic control systems. LAP LAMBERT Academic Publishing, Saarbrücken.

[12] Shafi, U., Mumtaz, R., García-Nieto, J., Hassan, S. A., Zaidi, S. A. R., & Iqbal, N. (2019). Precision agriculture techniques and practices: From considerations to applications. Sensors, 19(17), 3796.

[13] Cobbenhagen, A. T. J. R., Antunes, D. J., Van De Molengraft, M. J. G., & Heemels, W. P. M. H. (2021). Opportunities for control engineering in arable precision agriculture. Annual Reviews in Control, 51, 47-55.

[14] Waleed, M., Um, T. W., Kamal, T., Khan, A., & Iqbal, A. (2020). Determining the precise work area of agriculture machinery using internet of things and artificial intelligence. Applied Sciences, 10(10), 3365.

[15] Wang, P., Yue, M., Yang, L., Luo, X., He, J., Man, Z., ... & Hu, L. (2024). Design and test of intelligent farm machinery operation control platform for unmanned farms. Agronomy, 14(4), 804.

[16] Che, Y., Zheng, G., Li, Y., Hui, X., & Li, Y. (2024). Unmanned Agricultural Machine Operation System in Farmland Based on Improved Fuzzy Adaptive Priority-Driven Control Algorithm. Electronics, 13(20), 4141.

[17] Wang, C., An, Z., Jairueng, S., Ruekkasaem, L., Jayasudha, M., & Singh, B. K. (2022). Model Optimization of Agricultural Machinery Information Control System Based on Artificial Intelligence. Journal of Food Quality, 2022(1), 7456650.

[18] Ni, J. (2023). Precision Operation Technology and Intelligent Equipment in Farmland. Agronomy, 13(11), 2721.

[19] Wang, B., Du, X., Wang, Y., & Mao, H. (2024). Multi-machine collaboration realization conditions and precise and efficient production mode of intelligent agricultural machinery. International Journal of Agricultural and Biological Engineering, 17(2), 27-36.

[20] Akintuyi, O. B. (2024). Adaptive AI in precision agriculture: a review: investigating the use of self-learning algorithms in optimizing farm operations based on real-time data. Research Journal of Multidisciplinary Studies, 7(02), 016-030.